The application of Bryan Baum's VIIRS CrIS data fusion spectral files

Steven Massie

Laboratory for Atmospheric and Space Physics (LASP)

University of Colorado

Libera Science Team Meeting

November 16, 2020

Main Points

This talk is in response to what was said and learned from the recent CERES Science Team meeting, and in response to several of Peter's statements expressed during the past several months.

Goal of the talk: put CrIS and its capabilities "on our radar screens"

Point out the utility of Bryan Baum's data files which contain VIIRS and CrIS spectra (and which are already in production).

Libera, VIIRS, and CrIS will co-fly on JPSS-3.

a) The VIIRS and CrIS spectra could be helpful in the Libera "unfiltering" algorithm / algorithm validation calculations.

b) The VIIRS and CrIS spectra could also be useful as a development resource for "hyperspectral" instrument development as applied to Earth Radiation Budget studies.

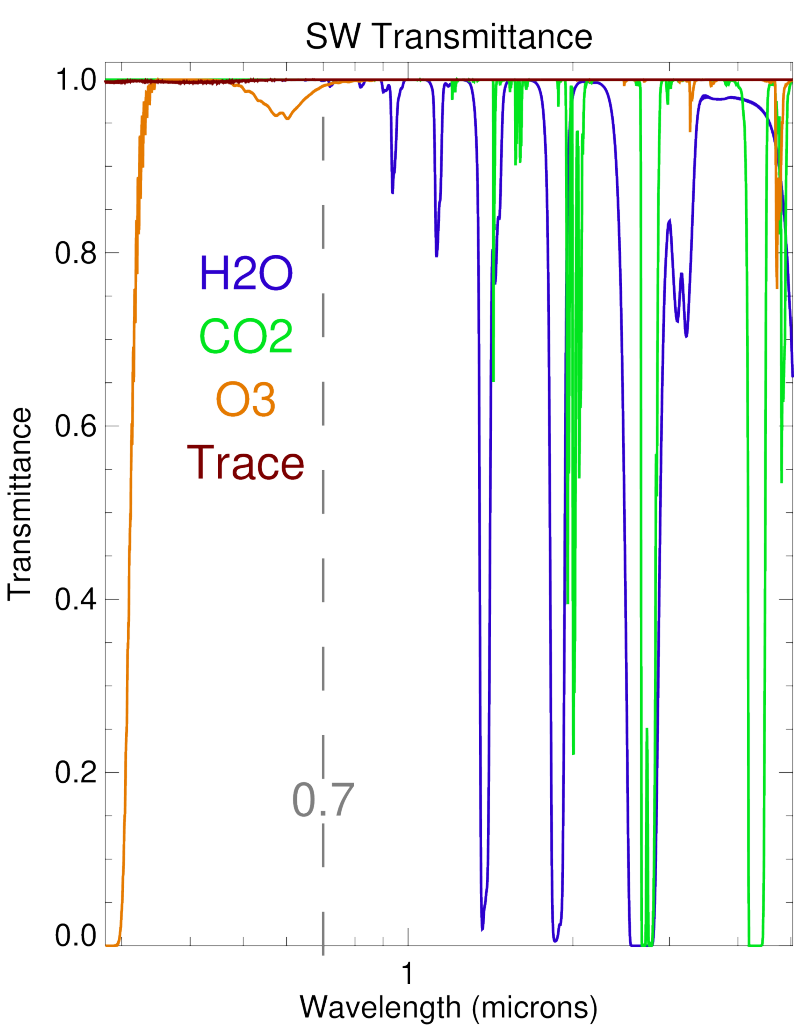

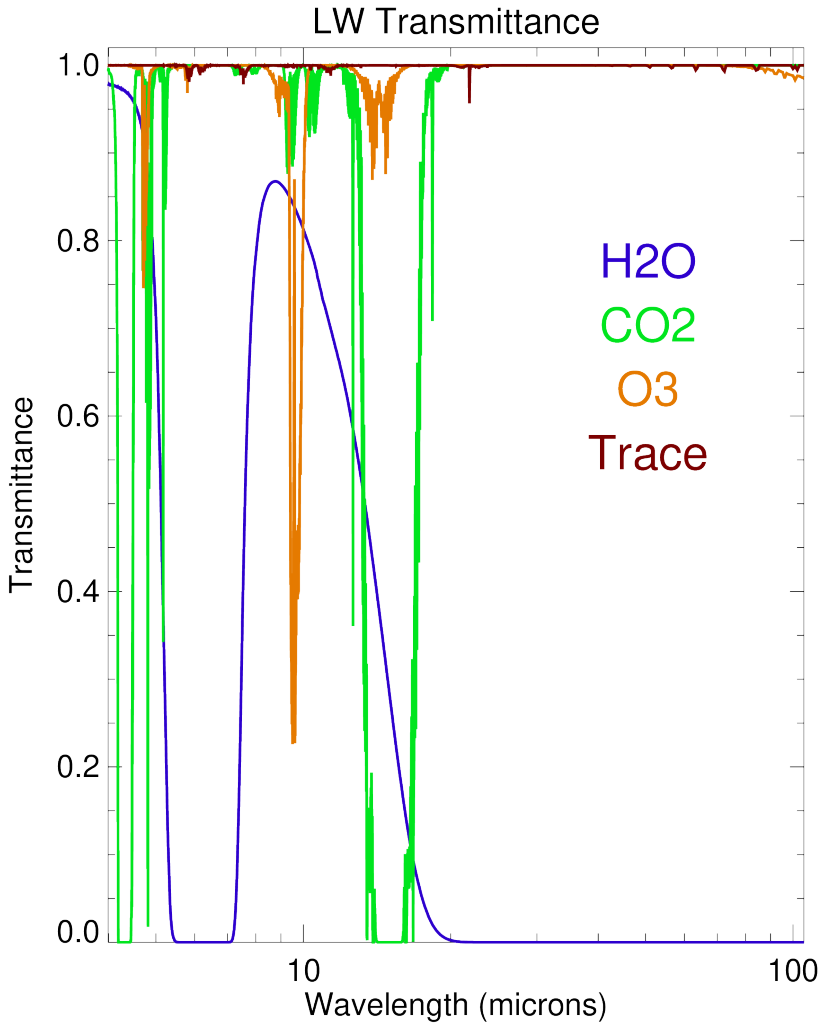

0.3 **0.7** **5** **5** **10** **100**

Review of the spectral territory based on representative MODTRAN 6 calculations
There are many constituents / factors which modulate transmission at the 0.1 % level

Review of where the information comes from

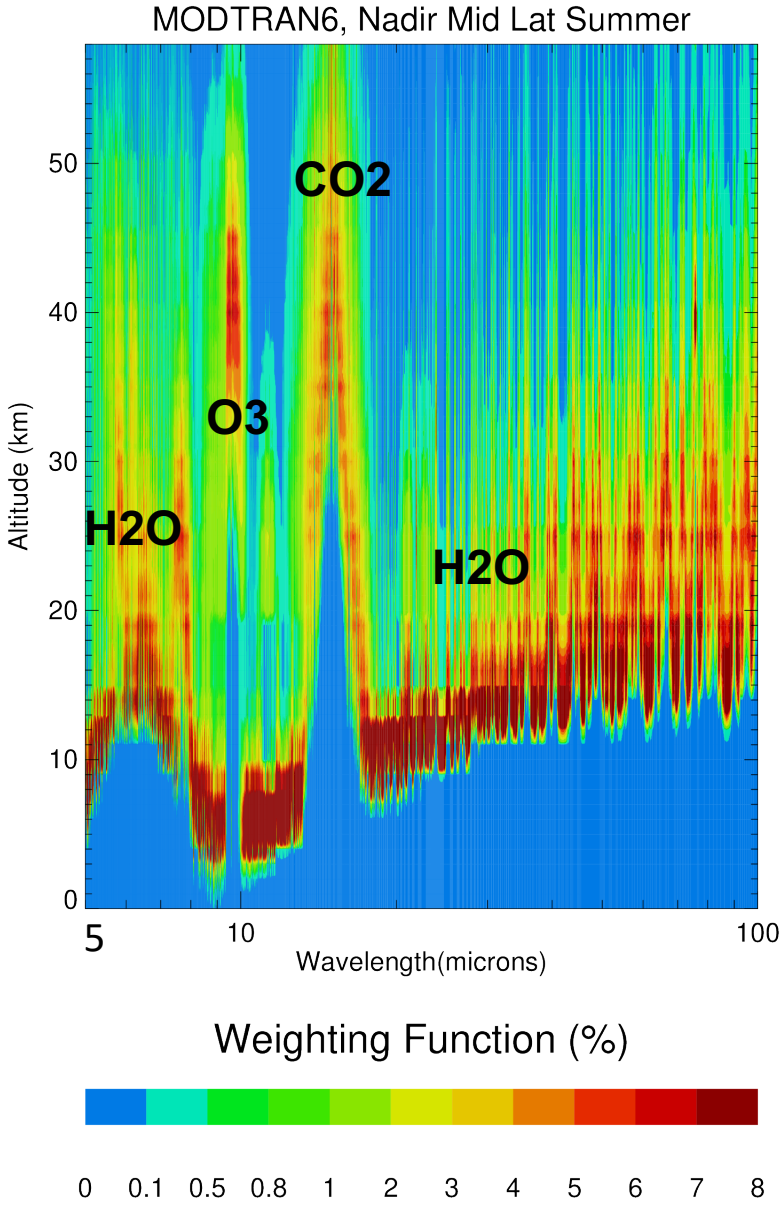

Weighting function, W((λ,z)

W(λ,z) =100 { B(λ,T) exp(-τ(z,∞)) dτ } / rad

with rad = ∫ B(λ,T) exp(-τ) dτ

and temperature T

A wide range of altitude contributes to the top of atmosphere radiances

To understand how and where (altitude wise) the radiances come from you need an instrument that can probe the altitudes of interest (CrIS is helpful for this)

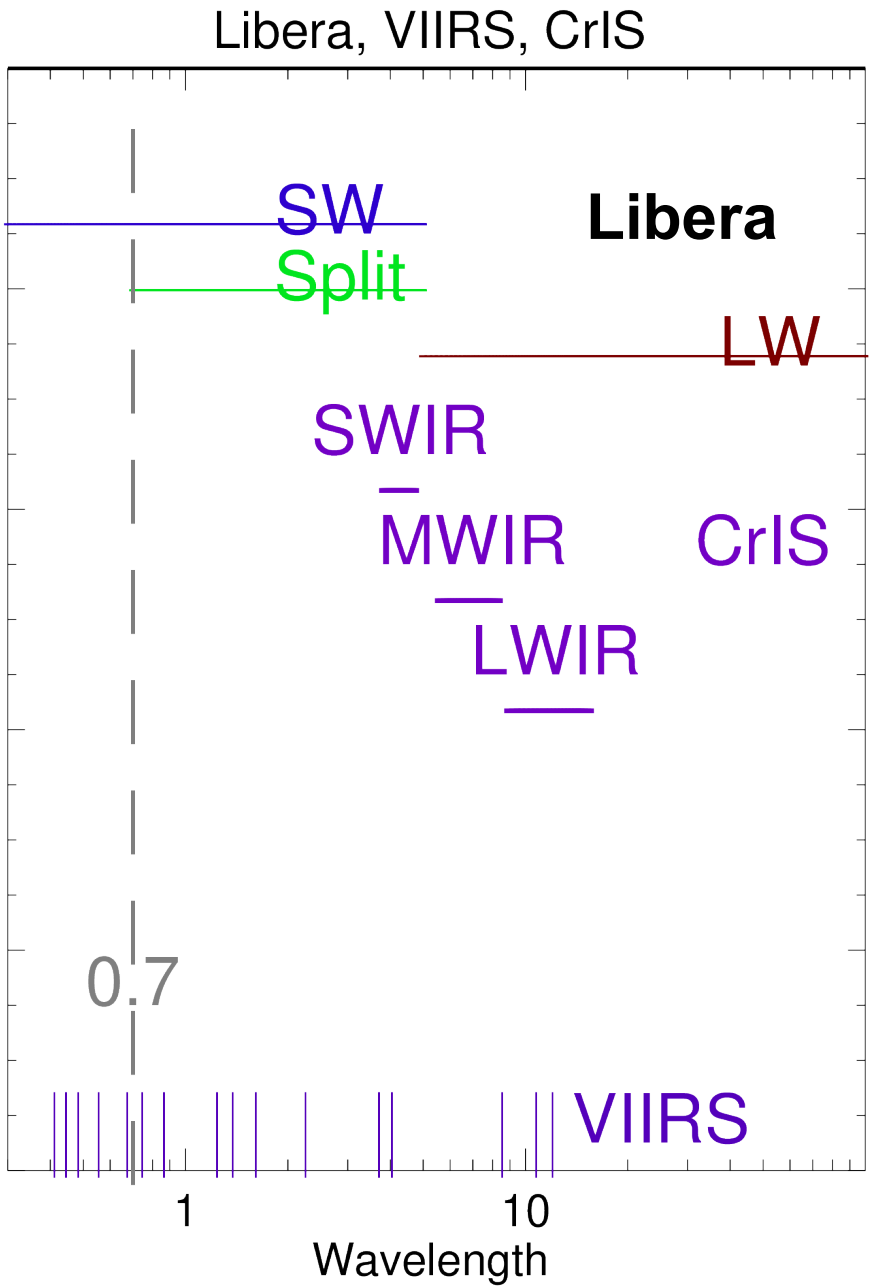

1305 spectral channels

Molecular Contributions to Spectrum

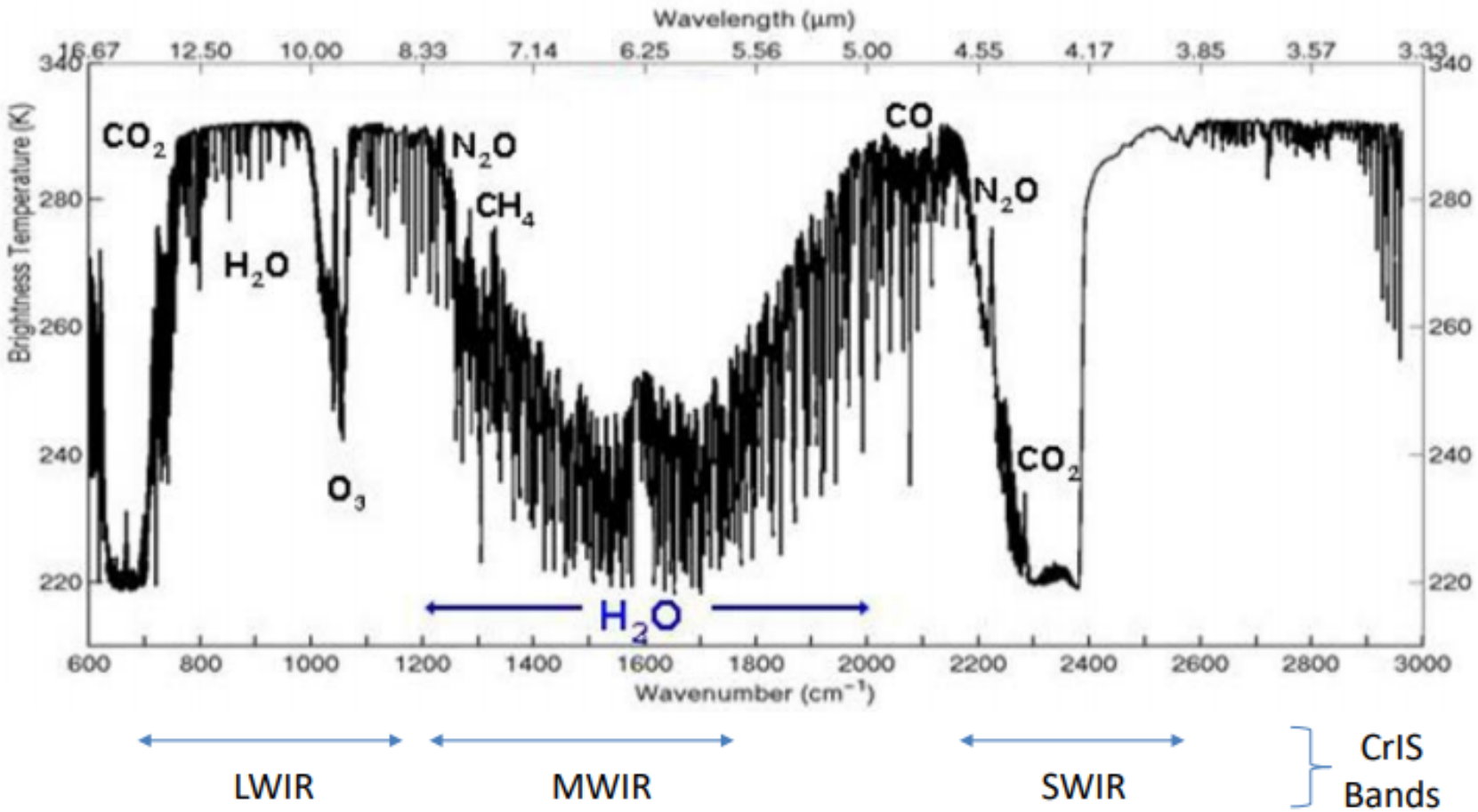

Data Inter-comparisons of the CRIS Interferometers on SUOMI-NPP and NOAA-20
Joe Kristl, Kori Moore, Mark Esplin, Deron Scott, 20 June 2018

VIIRS (0.4 – 12 μm)

		Specification									
		Band No.	Driving EDR(s)	Spectral Range (um)	Horiz Sample Interval (km) (track x Scan) Nadir	End of Scan	Band Gain	Ltyp or Ttyp (Spec)	Lmax or Tmax	SNR or NEdT (K)	Measured SNR or NEdT (K)	SNR Margin (%)
Reflective Bands	VisNIR	M1	Ocean Color Aerosol	0.402 - 0.422	0.742 x 0.259	1.60 x 1.58	High Low	44.9 155	135 615	352 316	723 1327	105% 320%
		M2	Ocean Color Aerosol	0.436 - 0.454	0.742 x 0.259	1.60 x 1.58	High Low	40 146	127 687	380 409	576 1076	51.5% 163%
		M3	Ocean Color Aerosol	0.478 - 0.498	0.742 x 0.259	1.60 x 1.58	High Low	32 123	107 702	416 414	658 1055	58.2% 155%
		M4	Ocean Color Aerosol	0.545 - 0.565	0.742 x 0.259	1.60 x 1.58	High Low	21 90	78 667	362 315	558 882	54.1% 180%
		I1	Imagery EDR	0.600 - 0.680	0.371 x 0.387	0.80 x 0.789	Single	22	718	119	265	122.7%
		M5	Ocean Color Aerosol	0.662 - 0.682	0.742 x 0.259	1.60 x 1.58	High Low	10 68	59 651	242 360	360 847	49% 135%
		M6	Atmosph. Correct.	0.739 - 0.754	0.742 x 0.776	1.60 x 1.58	Single	9.6	41	199	394	98.0%
		I2	NDVI	0.846 - 0.885	0.371 x 0.387	0.80 x 0.789	Single	25	349	150	299	99.3%
		M7	Ocean Color Aerosol	0.846 - 0.885	0.742 x 0.259	1.60 x 1.58	High Low	6.4 33.4	29 349	215 340	545 899	154% 164%
	S/WMIR	M8	Cloud Particle Size	1.230 - 1.250	0.742 x 0.776	1.60 x 1.58	Single	5.4	165	74	349	371.6%
		M9	Cirrius/Cloud Cover	1.371 - 1.386	0.742 x 0.776	1.60 x 1.58	Single	6	77.1	83	247	197.6%
		I3	Binary Snow Map	1.580 - 1.640	0.371 x 0.387	0.80 x 0.789	Single	7.3	72.5	6	165	2650.0%
		M10	Snow Fraction	1.580 - 1.640	0.742 x 0.776	1.60 x 1.58	Single	7.3	71.2	342	695	103.2%
		M11	Clouds	2.225 - 2.275	0.742 x 0.776	1.60 x 1.58	Single	0.12	31.8	10	18	80.0%
Emissive Bands		I4	Imagery Clouds	3.550 - 3.930	0.371 x 0.387	0.80 x 0.789	Single	270	353	2.5	0.4	84.0%
		M12	SST	3.660 - 3.840	0.742 x 0.776	1.60 x 1.58	Single	270	353	0.396	0.12	69.7%
		M13	SST Fires	3.973 - 4.128	0.742 x 0.259	1.60 x 1.58	High Low	300 380	343 634	0.107 0.423	0.044 --	59% --
	LWIR	M14	Cloud Top Properties	8.400 - 8.700	0.742 x 0.776	1.60 x 1.58	Single	270	336	0.091	0.054	40.7%
		M15	SST	10.263 - 11.263	0.742 x 0.776	1.60 x 1.58	Single	300	343	0.07	0.028	60.0%
		I5	Cloud Imagery	10.500 - 12.400	0.371 x 0.387	0.80 x 0.789	Single	210	340	1.5	0.41	72.7%
		M16	SST	11.538 - 12.488	0.742 x 0.776	1.60 x 1.58	Single	300	340	0.072	0.036	50.0%

0.742 x 0.259 km

Visible Infrared Imaging Radiometer Suite (VIIRS) Sensor Data Record (SDR) User's Guide, March 2017

Bryan Baum's files

Each file (size ~ 200 Mb) covers a 6 minute region

Visible Infrared Imaging Radiometer Suite (VIIRS)
CrIS (Cross-track Imager Sounder)

The data files specify radiances at VIIRS M-band resolution (750m)

CrIS specs:

- **Has AIRS-like capabilities**
  - **AIRS gives excellent temperature profile information**
- **2200 km swath, 1305 spectral bands, 1.1 to 4.5 cm^{-1} resolution**
- **Field of View (FOV): Nadir 14 km**

Bryan takes the CrIS spectra and applies the MODIS filter functions to produce a set of MODIS-like radiances.

He does all of the VIIRS – CrIS co-location calculations.

Bryan Baum's files

Question: How can 14 km spatial resolution CrIS observations be used to create a 0.7 km field of view data product?

Asked Bryan this question. Key points of his response:

"There are 2 parts to the fusion process.
The first step is primarily one of geolocation between VIIRS and CrIS.

A k-d tree analysis provides the index of 5 CrIS FOVs that best match the high / low resolution VIIRS 11/12 um radiances

In the 2nd step of the process, the CrIS spectra are convolved according to our defined Aqua MODIS spectral response functions."

Question: Do the VIIRS – CrIS colocation match-ups have the same instrument pointing geometry?

If the sensor zenith and sensor azimuth angles are not the same for Libera, VIIRS, or CrIS, then a co-added set of VIIRS and CrIS radiances are Very Problematic !

The Libera "Unfiltering" Process – a suggested approach

Example: Libera Split Window *spectral response function* $F(\lambda)$ for the 0.7 to 5.0 μm range Alas, $F(\lambda) < 1.0$

$R(\lambda)$ = actual top of atmosphere *spectral radiance*, W m^{-2} μm^{-1} $ster^{-1}$

Define the *split window radiance* as S, W m^{-2} $ster^{-1}$

$$S = \int R(\lambda)\, d\lambda$$

***Measured radiance* SF(obs) = $\int R(\lambda)\, F(\lambda)\, d\lambda < S$**

The ratio S / SF is > 1. We need to calculate S / SF as accurately as possible.

The ratio S / SF is calculated utilizing a *proxy* R'(λ) derived from a *combination* of (and perhaps guided by *machine learning* smarts)

- **Libera camera information (to identify scene context)**
- **Dan Feldman's OSSE library of calculated spectra and scenes**
- **Baum's VIIRS and CrIS data fusion files**

The Libera value of S is then SF(obs) $\int R'(\lambda)\, d\lambda$ / $\int R'(\lambda)\, F(\lambda)\, d\lambda$

For a single CERES observation, co-added spectra within a 24 km circle

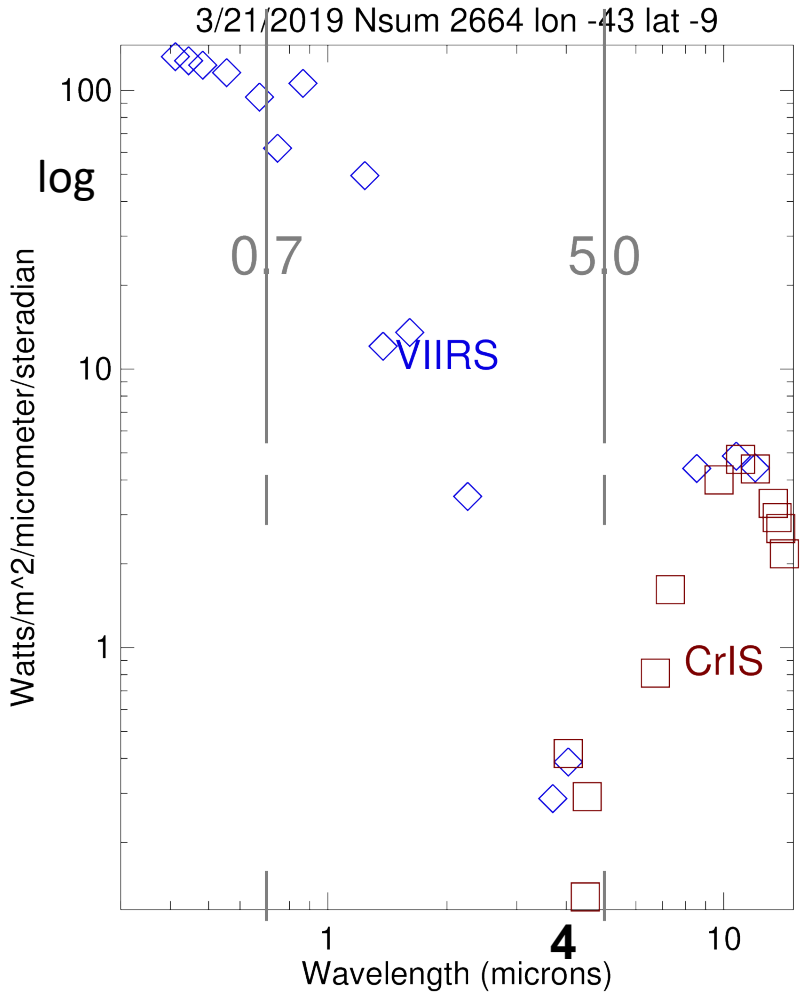

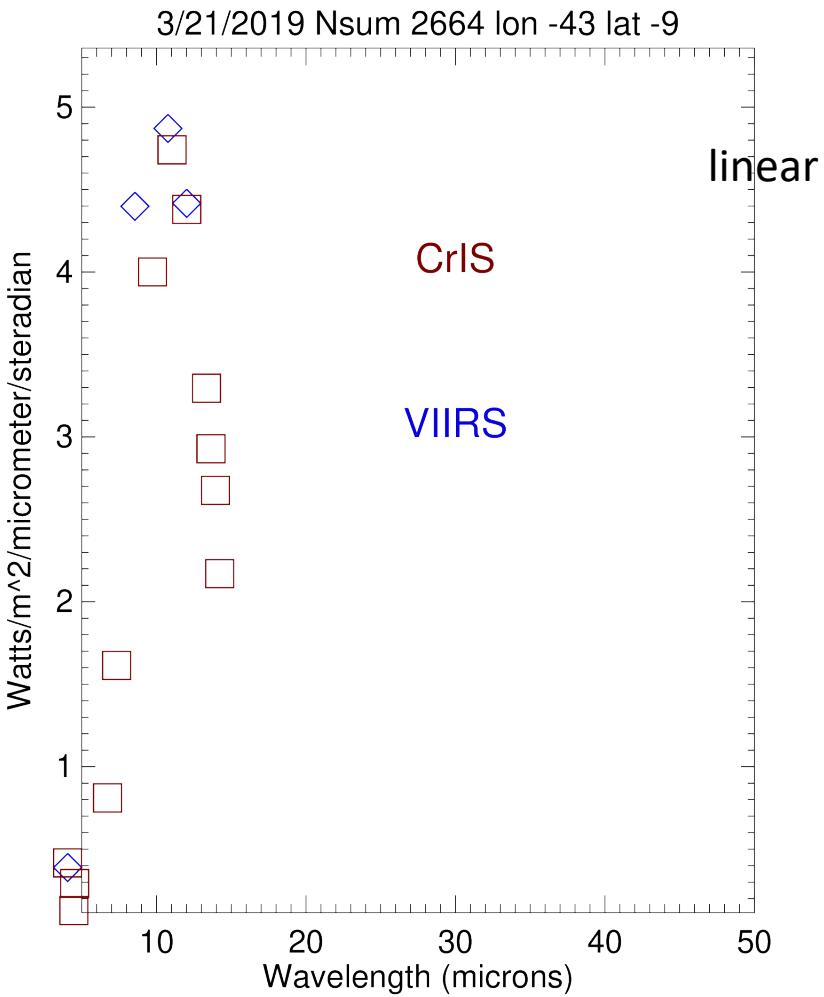

For a representative 24 km FOV, 2664 VIIRS and CrIS spectra are co-added.
But there is a tremendous amount of radiance variations in a 24 km circle!
stnd dev of VIIRS radiance variations within a 24 km circle are 34 % and 52 % at 12.02 μm and 4.05 μm (wavelengths that are common to VIIRS and CrIS)
At 4.05 μm the 95% confidence of the determination of the VIIRS average is 2%

How well do CrIS data fusion radiances *track* VIIRS sub-1 km radiances?

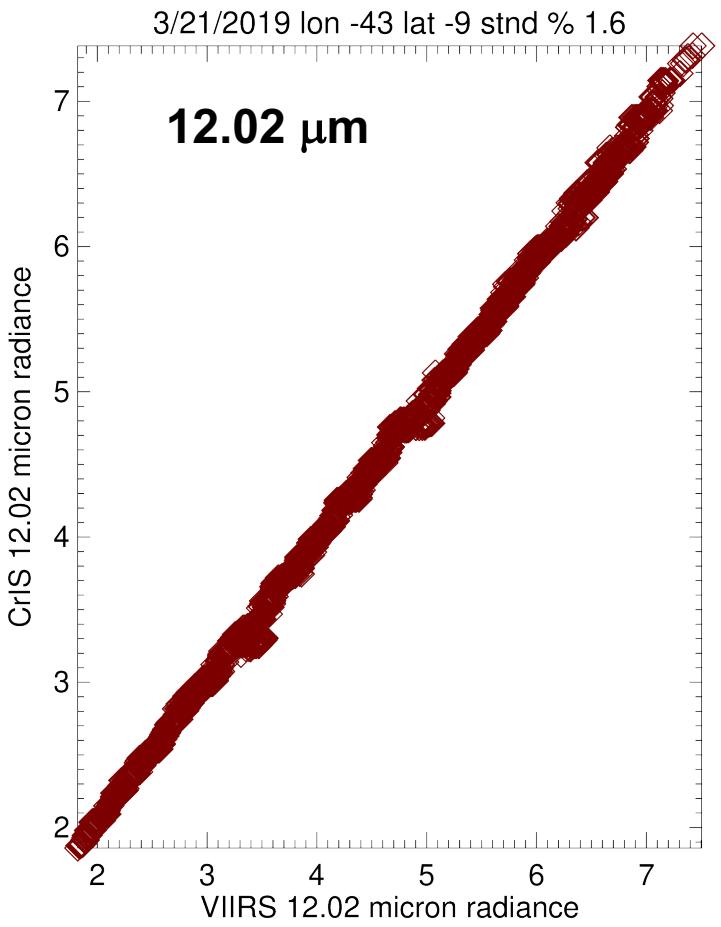

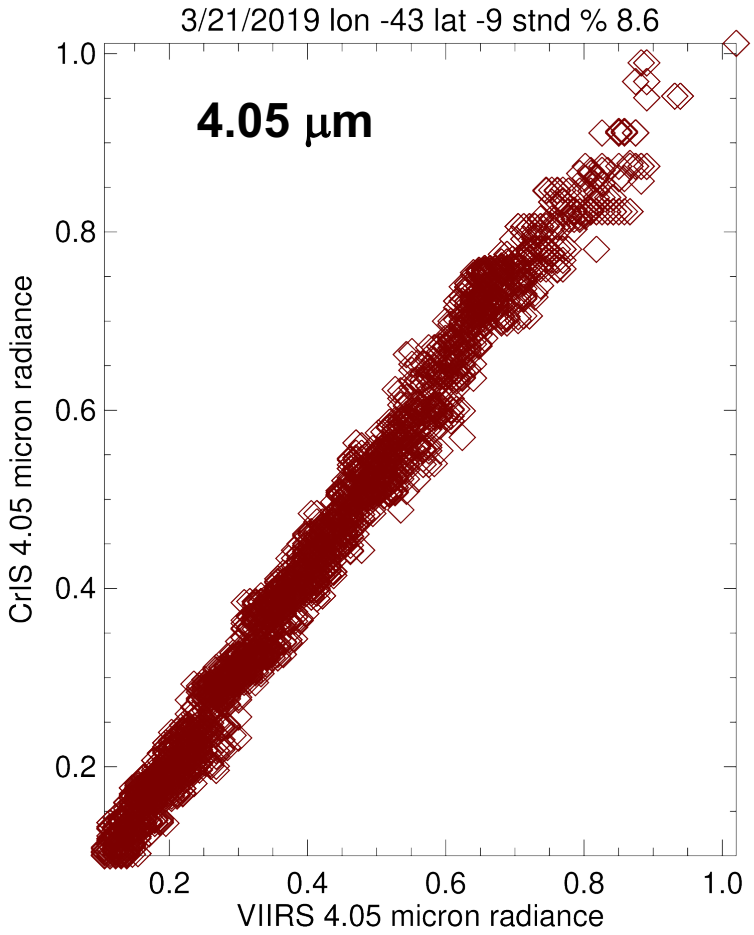

Stnd deviation of 100 (CrIS – VIIRS)/ ave = 1.6 % Stnd deviation at 4.05 μm = 8.6 %
for CrIS and VIIRS radiances within a 24 km averaging circle

My concern: you may get close agreement between CrIS and VIIRS radiances at 12 μm, but there are sub-1km variations in CrIS-VIIRS at 4 μm

Error sensitivity for S / SF = $\int R'(\lambda)\, d\lambda \;/\; \int R'(\lambda)\, F(\lambda)\, d\lambda$

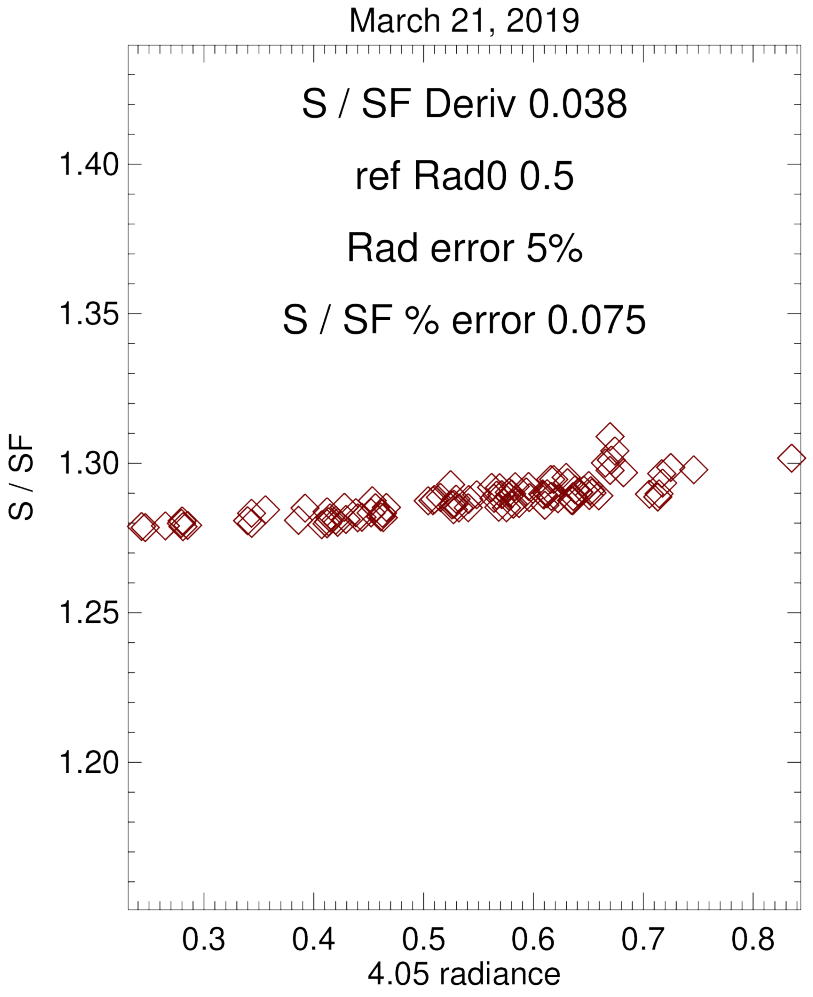

R'(λ) top of atmosphere spectral radiance
W m^{-2} μm^{-1} ster^{-1}

F(λ) spectral response function

R' is based on averaging ~2500 CrIs – VIIRS spectra in a 24 km circle surrounding a CERES observation point.
Did this for 100 R' cases over the cloudy Amazon.

If the 4 μm radiance is uncertain by 5%, then the "unfiltering" S / SF calculation for the split window has a 0.075 % error

Libera Science Goal

"Develop techniques to utilize hyper-spectral instrumentation to better understand Earth's radiation budget"

CrIS and VIIRS data (from SOUMI - NPP) can be used in Odele's BABAR-ERI *follow-on instrument* concept designs.

Take the CrIS spectra (with 1305 data points), and produce narrow band integrated radiances for instrument concepts observing the H_2O (6 μm) and O_3 (9.6 μm) bands

Concluding Remarks

Bryan Baum was asked at the summer 2020 CERES Science Team meeting if the production of the VIIRS – CrIS data fusion files is a long term certainty.

He replied “no”.

If these data files (in the setting of JPSS-3 in 2027) are recognized to be of importance to Libera, then we need to advise NASA to make sure that such files are available during the Libera mission.

Extra Slides

Data courtesy of LARC's Kory Priestley

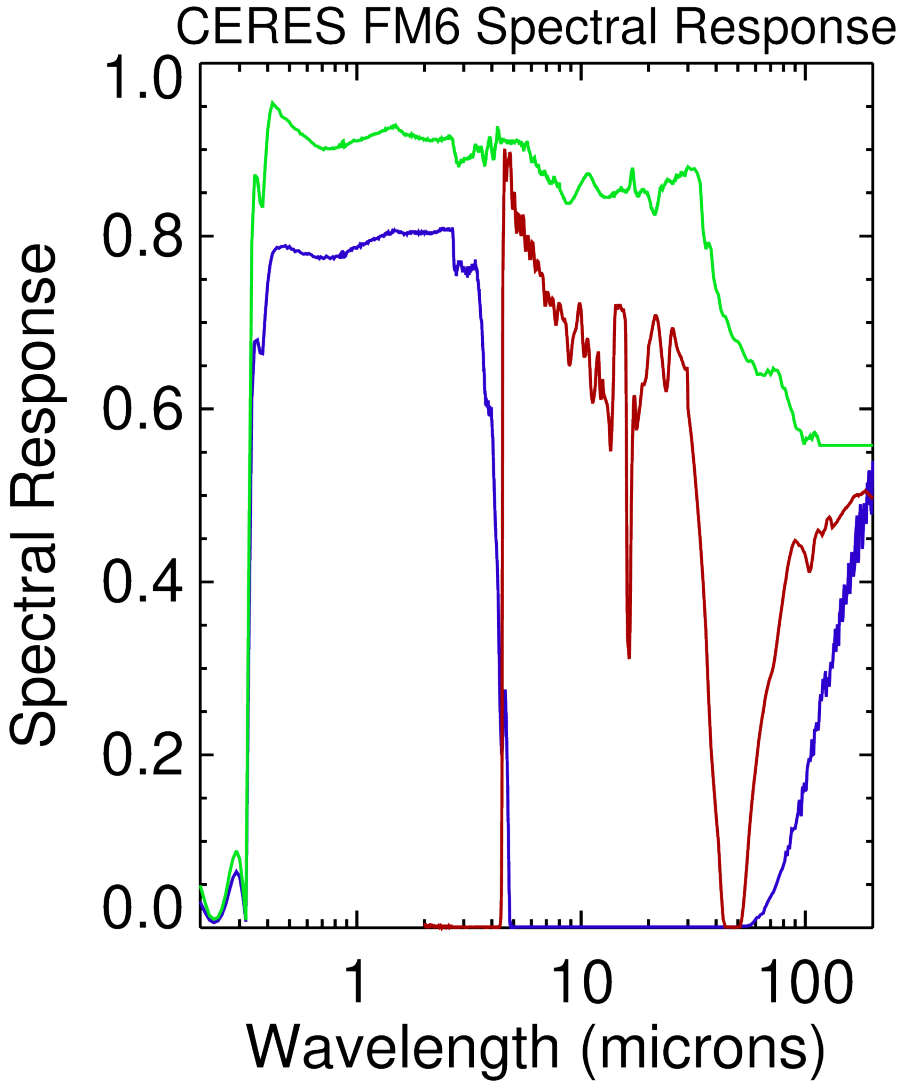

Filter response deviates from unity by a lot !

Used the blue curve for the 0.7 to 5 μm S / SF sensitivity calculation.

Table 1: MODIS and VIIRS infrared (IR) bands.

MODIS Infrared bands		VIIRS Infrared bands		Primary Use
band	Central Wavelength [μm]	band	Central Wavelength [μm]	
23	4.05	M13	4.05	Atmospheric temperature
24	4.47			Atmospheric temperature
25	4.52			Atmospheric temperature
27	6.72			Water vapor
28	7.33			Water vapor
29	8.55	M14	8.55	Surface and cloud properties
30	9.73			Ozone
31	11.03	M15	10.76	Surface and cloud properties
32	12.02	M16	12.01	Surface and cloud properties
33	13.34			Cloud properties
34	13.64			Cloud properties
35	13.94			Cloud properties
36	14.23			Cloud properties

Fusion of VIIRS and CrIS data to construct infrared (IR) absorption band radiances for VIIRS Bryan A. Baum , W. P. Menzel , and E. Weisz, September 2019, ATBD

CrIS Interferometer on NOAA-20/SNPP

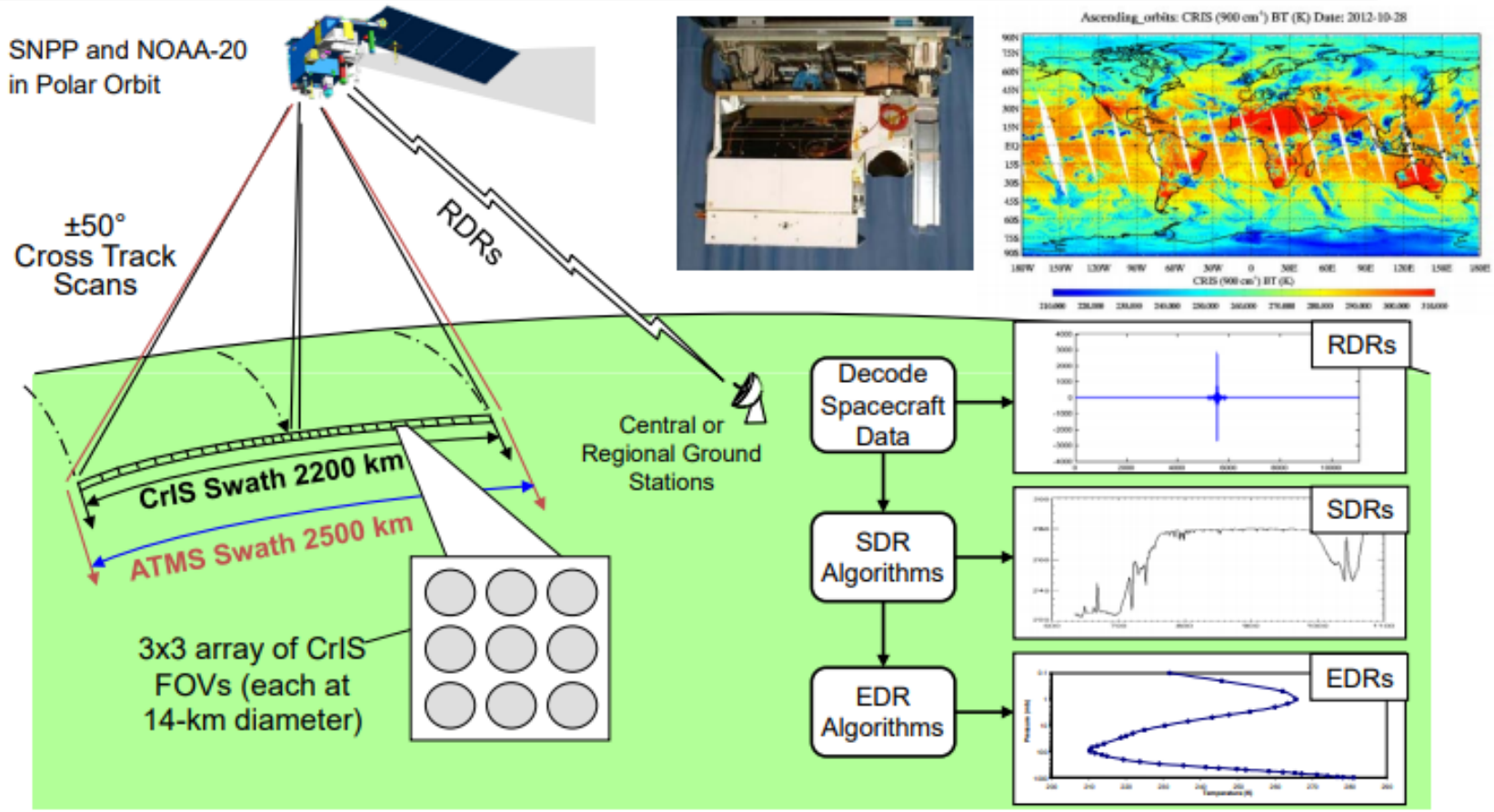

Data Inter-comparisons of the CRIS Interferometers on SUOMI-NPP and NOAA-20
Joe Kristl, Kori Moore, Mark Esplin, Deron Scott, 20 June 2018

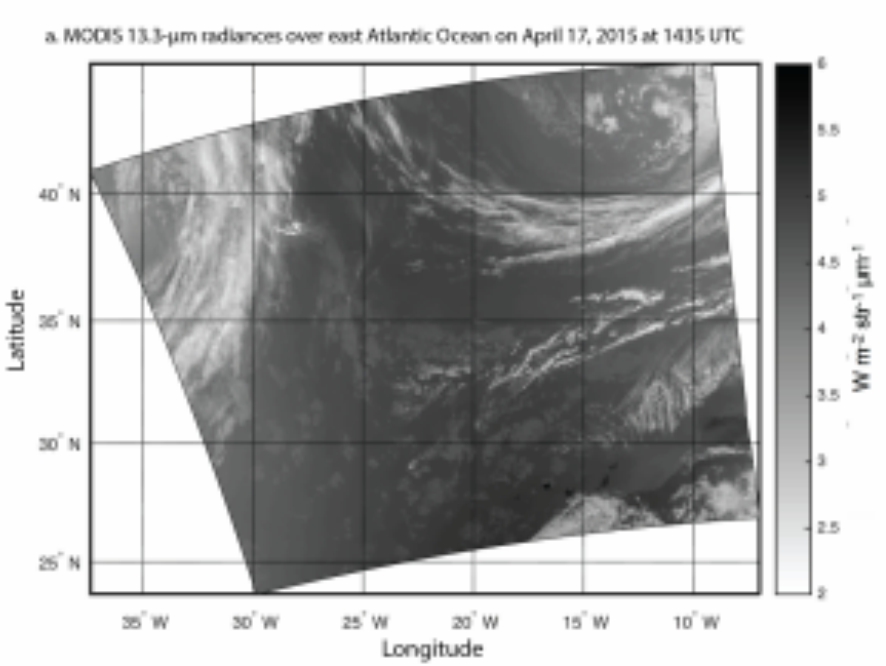

MODIS

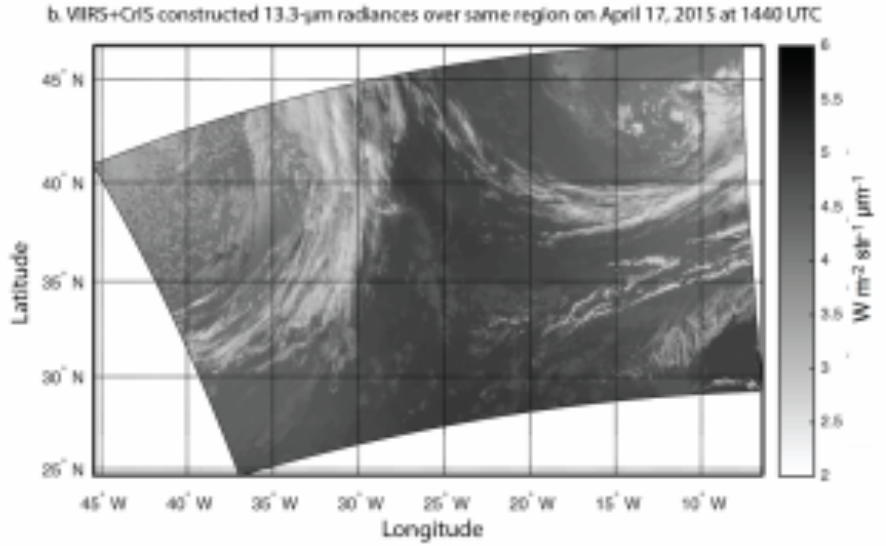

VIIRS + CrIS

Fusion of VIIRS and CrIS data to construct infrared (IR) absorption band radiances for VIIRS Bryan A. Baum , W. P. Menzel , and E. Weisz, September 2019, ATBD

Example of use of Bryan Baum's archived VIIRS-CrIS spectra

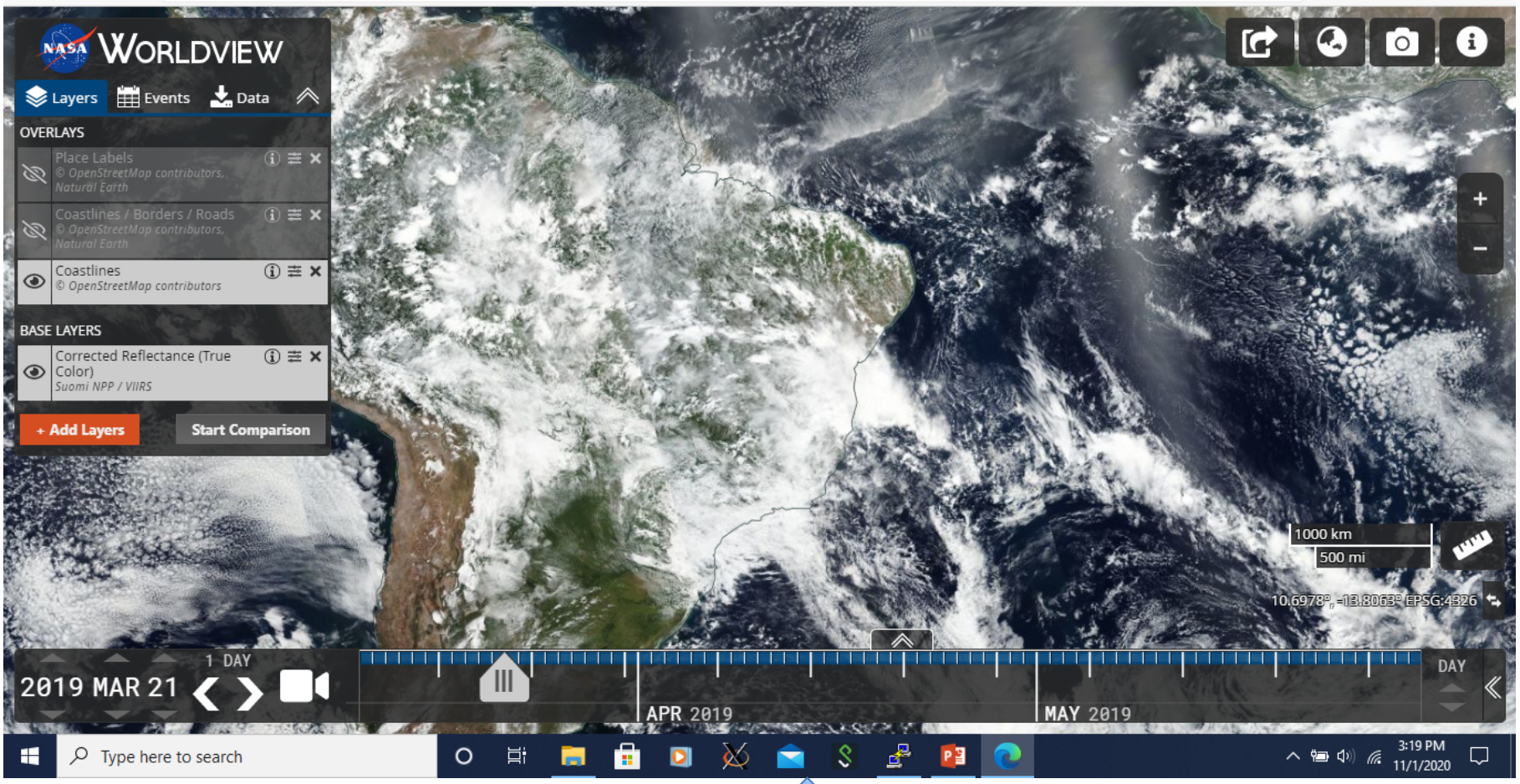

The co-added spectra for slide 11 pertain to a cloudy Amazon scene.

VIIRS Spectral Bands

0.4 μm

12.01

0.742 x 0.259 km

		Band No.	Wave-length (μm)	Horiz Sample Interval (km Downtrack x Crosstrack)		Driving EDRs	Radi-ance Range	Ltyp or Ttyp
				Nadir	End of Scan			
VIS/NIR FPA	Silicon PIN Diodes	M1	0.412	0.742 x 0.259	1.60 x 1.58	Ocean Color Aerosols	Low High	44.9 155
		M2	0.445	0.742 x 0.259	1.60 x 1.58	Ocean Color Aerosols	Low High	40 146
		M3	0.488	0.742 x 0.259	1.60 x 1.58	Ocean Color Aerosols	Low High	32 123
		M4	0.555	0.742 x 0.259	1.60 x 1.58	Ocean Color Aerosols	Low High	21 90
		I1	0.640	0.371 x 0.387	0.80 x 0.789	Imagery	Single	22
		M5	0.672	0.742 x 0.259	1.60 x 1.58	Ocean Color Aerosols	Low High	10 68
		M6	0.746	0.742 x 0.776	1.60 x 1.58	Atmospheric Corr'n	Single	9.6
		I2	0.865	0.371 x 0.387	0.80 x 0.789	NDVI	Single	25
		M7	0.865	0.742 x 0.259	1.60 x 1.58	Ocean Color Aerosols	Low High	6.4 33.4
CCD		DNB	0.7	0.742 x 0.742	0.742 x 0.742	Imagery	Var.	6.70E-05
SMWIR	PV HgCdTe (HCT)	M8	1.24	0.742 x 0.776	1.60 x 1.58	Cloud Particle Size	Single	5.4
		M9	1.378	0.742 x 0.776	1.60 x 1.58	Cirrus/Cloud Cover	Single	6
		I3	1.61	0.371 x 0.387	0.80 x 0.789	Binary Snow Map	Single	7.3
		M10	1.61	0.742 x 0.776	1.60 x 1.58	Snow Fraction	Single	7.3
		M11	2.25	0.742 x 0.776	1.60 x 1.58	Clouds	Single	0.12
		I4	3.74	0.371 x 0.387	0.80 x 0.789	Imagery Clouds	Single	270 K
		M12	3.70	0.742 x 0.776	1.60 x 1.58	SST	Single	270 K
		M13	4.05	0.742 x 0.259	1.60 x 1.58	SST Fires	Low High	300 K 380 K
LWIR	PV HCT	M14	8.55	0.742 x 0.776	1.60 x 1.58	Cloud Top Properties	Single	270 K
		M15	10.763	0.742 x 0.776	1.60 x 1.58	SST	Single	300 K
		I5	11.450	0.371 x 0.387	0.80 x 0.789	Cloud Imagery	Single	210 K
		M16	12.013	0.742 x 0.776	1.60 x 1.58	SST	Single	300 K

Rev. 062708

Table 1. VIIRS Band Centers, Spatial Resolution, and Gain[15] (note: HSI for dual gain bands are before

Visible Infrared Imaging Radiometer Suite (VIIRS) Sensor Data Record (SDR) User's Guide, March 2017

VIIRS Radiometric Uncertainty

Table: 3.1.5.9.2.3-1 Absolute radiometric calibration uncertainty of spectral radiance for moderate resolution emissive bands

Band	λc (μm)	Scene Temperature				
.	.	190K	230K	270K	310K	340K
M12	3.7	N/A	7.0%	0.7%	0.7%	0.7%
M13	4.05	N/A	5.7%	0.7%	0.7%	0.7%
M14	8.55	12.3%	2.4%	0.6%	0.4%	0.5%
M15	10.763	2.1%	0.6%	0.4%	0.4%	0.4%
M16	12.013	1.6%	0.6%	0.4%	0.4%	0.4%

Table: 3.1.5.9.2.4-1 Radiometric calibration uncertainty for imaging emissive bands

Band	Center Wavelength (nm)	Calibration Uncertainty
I4	3740	5.0%
I5	11450	2.5%

Cao, C., Suomi NPP VIIRS SDR Provisional Product Highlight, October, 2012

VIIRS Radiometric Uncertainty

VIIRS Rotating Telescope Assembly (RTA) Mirror Degradation

- VIIRS RTA mirror degradation continues as predicted (currently about ~30% in the 0.86 bands)
- Root cause of the degradation is traced to Tungsten/Tungsten oxide contamination in the manufacturing process prelaunch
- The impact of the responsivity degradation is mitigated through weekly calibration updates
- The remaining effect of the degradation is decreased signal to noise ratio, although its impact to products is still negligible

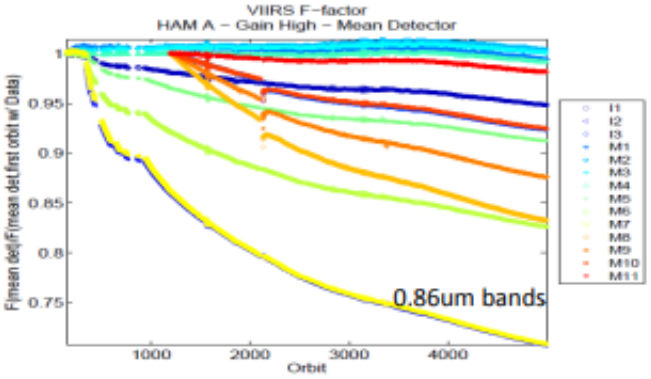

1

0.75

VIIRS RTA mirror degradation since launch

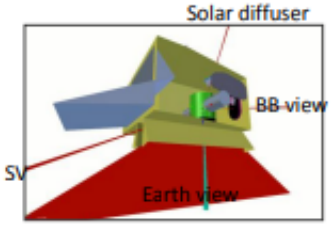

The VIIRS RTA degradation is quantified by its response to the onboard solar diffuser

Cao, C., Suomi NPP VIIRS SDR Provisional Product Highlight, October, 2012

VIIRS Radiometric Uncertainty

Cross Comparison with Aqua/MODIS

VIIRS		MODIS		Bias (V-M)×100%/M	
Band	Wavelength (μm)	Band	Wavelength (μm)	Ocean	Desert
M1	0.402 - 0.422	8	0.405 - 0.420	-2.0% ± 0.6%	-2.6% ± 0.7%
M2	0.436 - 0.454	9	0.438 - 0.448	**-4.0% ± 0.3%**	**-3.1% ± 0.8%**
M3	0.478 - 0.498	10	0.483 - 0.493	-1.1% ± 0.4%	-1.3% ± 0.6%
M4	0.545 - 0.565	4	0.545 - 0.565	**4.0% ± 0.8%**	-2.2% ± 0.6%
M5	0.662 - 0.682	1	0.620 - 0.670	**-5.6% ± 1.2%**	8.8% ± 0.7%
M6	0.739 - 0.754	15	0.743 - 0.753	-1.2% ± 1.7%	Saturate
M7	0.846 - 0.885	2	0.841 - 0.876	**-1.2% ± 1.2%**	2.3% ± 0.5%
M8	1.230 - 1.250	5	1.230 - 1.250		1.5% ± 0.5%

VIIRS Bands	Desert Bias(V-M)×100%/M		VIIRS Bands	Ocean Bias(V-M)×100%/M	
	Hyperion	*MODTRAN*		AVIRIS	*MODTRAN*
M1 (402m-422nm)		*1.50%*	M1 (402nm-422nm)	-1.10%	*-0.90%*
M2 (436nm-454nm)	0.28% ± 0.07%	*2.30%*	M2 (436nm-454nm)	0.50%	*0.40%*
M3 (478nm-498nm)	0.36% ± 0.08%	*0.70%*	M3 (478nm-498nm)	-0.45%	*-0.40%*
M4 (545nm-565nm)	0.47% ± 0.18%	*1.20%*	M4 (545nm-565nm)	1.10%	*0.80%*
M5 (662nm-682nm)	7.82% ± 0.02%	*9.80%*	M5 (662nm-682nm)	-1.70%	*-0.90%*
M6 (739nm-754nm)	Saturated		M6 (739nm-754nm)	-0.50%	*0.11%*
M7 (846nm-885nm)	2.68% ± 0.24%	*3.30%*	M7 (846nm-885nm)	3.50%	*4.00%*
M8 (1230nm-250nm)	4.80% ± 0.17%	*3.30%*			

Comparisons to Aqua/MODIS agree to 1 to 5 %

Cao, C., Suomi NPP VIIRS SDR Provisional Product Highlight, October, 2012

VIIRS Radiometric Uncertainty (NEdT)

Table 1. VIIRS Spectral Band Design Specifications and On-Orbit Performance (Radiance Unit: W/m^2/μm/sr)

FPA	Band No.	Spectral Range (μm)	Band Gain	Ltyp or Ttyp (K) Spec	Lmax or Tmax	SNR or NEdT (K) Spec	SNR or NEdT/Spec (Prelaunch)	SNR or NEdT/Spec (02/06/2012)	SNR or NEdT/Spec (05/22/2012)	SNR or NEdT/Spec (09/10/2012)	SNR or NEdT/Spec (12/17/2012)	SNR or NEdT/Spec (03/18/2013)
VIS/NIR	M1	0.402–0.422	High	44.9	135	352	1.75	1.69	1.70	1.66	1.70	1.72
			Low	155	615	316	3.46	3.37	3.34	3.32	3.42	3.54
	M2	0.436–0.454	High	40	127	380	1.64	1.54	1.56	1.53	1.57	1.56
			Low	146	687	409	2.73	2.58	2.54	2.53	2.62	2.63
	M3	0.478– 0.498	High	32	107	416	1.66	1.53	1.56	1.54	1.57	1.54
			Low	123	702	414	2.68	2.49	2.50	2.45	2.50	2.54
	M4	0.545–0.565	High	21	78	362	1.61	1.50	1.54	1.49	1.54	1.50
			Low	90	667	315	3.06	2.72	2.83	2.78	2.89	2.77
	I1	0.600–0.680	Single	22	718	119	2.02	1.79	1.77	1.76	1.76	1.76
	M5	0.662–0.682	High	10	59	242	1.51	1.37	1.33	1.35	1.34	1.30
			Low	68	651	360	2.30	1.74	1.68	1.69	1.68	1.65
	M6	0.739–0.754	Single	9.6	41	199	2.09	1.82	1.74	1.74	1.70	1.69
	I2	0.846–0.885	Single	25	349	150	2.03	1.72	1.61	1.55	1.52	1.50
	M7	0.846–0.885	High	6.4	29	215	2.42	2.08	1.97	1.87	1.84	1.80
			Low	33.4	349	340	2.49	1.83	1.68	1.61	1.57	1.53
S/MWR	M8	1.230–1.250	Single	5.4	165	74	3.69	3.10	2.84	2.73	2.65	2.60
	M9	1.371–1.386	Single	6	77.1	83	3.05	2.79	2.64	2.54	2.50	2.47
	I3	1.580–1.640	Single	7.3	72.5	6	28.67	25.48	24.49	24.12	23.75	23.58
	M10	1.580–1.640	Single	7.3	71.2	342	2.09	1.74	1.68	1.68	1.65	1.60
	M11	2.225–2.275	Single	0.12	31.8	10	2.50	2.21	2.21	2.16	2.15	2.14
	I4	3.550–3.930	Single	270 (K)	353	2.5 (K)	0.16	0.16	0.16	0.16	0.16	0.16
	M12	3.610–3.790	Single	270 (K)	353	0.396 (K)	0.33	0.33	0.33	0.33	0.28	0.30
	M13	3.973–4.128	High	300 (K)	343	0.107 (K)	0.37	0.37	0.37	0.37	0.37	0.37
			Low	380 (K)	634	0.423 (K)	N/A	N/A	N/A	N/A	N/A	N/A
LWR	M14	8.400–8.700	Single	270 (K)	336	0.091 (K)	0.66	0.55	0.66	0.66	0.66	0.66
	M15	10.263–11.263	Single	300 (K)	343	0.07 (K)	0.43	0.43	0.43	0.43	0.43	0.43
	I5	10.500–12.400	Single	210 (K)	340	1.5 (K)	0.27	0.27	0.27	0.27	0.27	0.27
	M16	11.538–12.488	Single	300 (K)	340	0.072 (K)	0.56	0.42	0.42	0.42	0.42	0.42

Xiong, et al. VIIRS on-orbit calibration methodology and performance, JGR, 2014